

Magnetic field noise analyses generated by the interactions between a nitrogen vacancy center diamond and surface and bulk impurities

Philip Chrostoski^{*,†,‡}, Bruce Barrios^{*}, D. H. Santamore^{*}

^{*}*Department of Physics and Engineering Physics, Delaware State University, Dover, DE 19901, USA*

[†]*Department of Physics and Astronomy, University of Missouri St. Louis, St. Louis, MO 63121, USA*

[‡]*Department of Physics, Missouri University of Science and Technology, Rolla, MO 65409, USA*

Abstract

We investigated the mechanism of magnetic noise due to both surface and bulk impurities. For surface noise, we apply the Langevin method to spin fluctuation theory to calculate the noise for paramagnetic surface impurities absorbed in a thin layer of water. We find that the mechanisms generating noise are spin flip and spin precession which depend on impurity spin relaxation and spin precession time. For the bulk noise, we consider carbon-13 and nitrogen as impurities and employ the correlated-cluster expansion to calculate noise. Carbon-13 noise is a few orders of magnitude larger than nitrogen due to the higher impurity density in the typical NV center diamond system. We also find that the noise in the secular approximation underestimates noise under low applied magnetic field. Overall, the major source of magnetic field noise is spin precession noise, which is more than five orders of magnitude larger than the spin flip noise.

Keywords: magnetic noise, NV center diamond

1. Introduction

Nitrogen vacancy (NV) center diamonds have recently emerged as promising candidates for nanoscale sensors, because of the long quantum coherence times of their spin states well above room temperature [1] and because of their high sensitivity to external magnetic and electric fields [2, 3] both at room temperature [4, 5, 6] and at very low temperatures [7]. These features have led to the use of NV centers as magnetic and electric field sensors [2, 3, 8], quantum information [9], magnetic imaging [10, 11], high spatial resolution devices [12] biomarkers [13], and temperature sensors [14, 15]. As a result, NV centers are a subject of intensive research, not only in physics, but also in chemistry [16, 17, 18], life science [19], and planetary studies [20].

One of the current serious problems is noise, which reduces sensitivity of NV center diamond sensors by broadening of the spectral linewidth and reduces spectral resolution of the device [21, 22]. Noise in NV center diamonds has two sources, the electric and magnetic fields. In some crystals used for optical device applications, crystal field splitting can produce Fano noise from charge fluctuations that contributes to the electric field noise [23, 24, 25]. In previous work we studied the electric field noise and found that surface electric field noise comes from surface charge fluctuations where the surface covering layer is the key to controlling this type of noise [26].

In this paper, we study magnetic field noise in an NV center diamond. This noise arises from interactions of the NV center electron spin with impurity spins in the system. The relevant impurities can occur both on the surface [27, 28, 29] and in the bulk [30]. We treat the surface impurity interactions in Sec. 2, and the bulk impurity interactions in Sec. 3.

The surface impurities we consider are absorbed molecules in a condensed thin layer of water that can hop around randomly among the terminated surface sites. We investigate hydrogen (H-), oxygen (O-), and fluorine (F-) terminated systems, since these are commonly used in NV center experiments where the noise reduction effects have been observed experimentally [31, 32, 33, 34], but the mechanisms and the key controlling factors of noise generation have never been investigated theoretically.

There are two mechanisms for NV center electron spin fluctuations that can contribute to the magnetic field noise: (a) fluctuations associated with the spin precession and (b) fluctuations due to spin flips. We model the noise using the Langevin method applied to the Bloch equation [35, 36, 37, 38]. We obtain the noise spectra by using the Langevin approach to spin fluctuation theory for all three different terminations.

We then study two typical bulk impurities in NV center diamonds: (a) carbon-13 isotopes that occur naturally and constitute 1% of the carbon atoms in the diamond; and (b) nitrogen atoms that remain after ion implantation during the production of the NV centers [39, 40]. Both species have nuclear spins that interact with the NV center electron spin, leading to magnetic field fluctuation noise [41, 42, 43]. We calculate the noise spectra using the correlated-cluster expansion method [44], which is particularly suited for dense systems of interacting particles [44, 45, 46]. We also examine the applicability of the secular approximation by comparing it with non-secular exact calculations.

In Sec. 4.1, we discuss the results of the surface impurity noise calculations. The O-terminated surface gives a much smaller noise floor than the other two terminated surfaces at the same amount of impurities. This is because of the very short (picosecond) spin-lattice relaxation time [47] of the impurity electron spins in the O-terminated system, compared to the H- and F-terminated systems, whose spin-lattice relaxation times are on the order of microseconds [48, 49].

A short relaxation time leads to a short impurity-impurity spin correlation time resulting in spin flip fluctuation noise only. On the other hand, a long relaxation time leads to a long impurity-impurity spin correlation time, which

results in activating another effect of spin-precession fluctuation noise to the already existing spin flip fluctuation noise. The spin precession fluctuation noise is larger than the spin flip fluctuation noise. The bonding between the hopping terminating atoms and the dangling bond will be reaction limited. This allows most of the sites above the NV center to be occupied by a terminating atom. At this point, the terminating atoms with long relaxation times are still generating spin precession noise. At high frequencies (short time scales), the spin precession is less prevalent as not enough time has passed for them to bond with dangling bonds.

The effective relaxation time is limited by whichever is faster of the spin-lattice relaxation rate or the “hopping” (i.e., the impurities moving around the surface) rate, yet the number of impurities affects only the hopping rate. Thus the relaxation time of H- and F-terminated surfaces transitions from being controlled by the hopping rate to being controlled by the spin flip rate as the impurity number increases. In contrast, the relaxation time of O-terminated surfaces is controlled by the spin flip rate for all practical levels of impurity incidence.

In Sec. 4.2, we discuss the results of the bulk impurity noise calculations. We find that the carbon-13 nuclear spin interaction is roughly two orders of magnitude larger than that of nitrogen. This is mainly because the number density of carbon in NV center diamonds exceeds that of nitrogen. As a result, the spacing between the NV center and the carbon-13 atoms will be smaller than the spacing between the NV center and the nitrogen atoms, resulting in a stronger interaction between the NV center and the carbon. In addition, the total fluctuations caused by the carbon-13 nuclear spin flip-flops are larger than those caused by the nitrogen nuclear spins.

The secular approximation, which is related to the rotating wave approximation, has been commonly used for the calculations of bulk impurity interactions as it is simpler and easy to evaluate. However, under low applied magnetic field ($B < 1$ G), we find that the secular approximation underestimates the amount of noise by a factor of 2.7. The secular approximation ignores the off-diagonal terms of the nuclear dipole-dipole interaction matrix, which is a valid assumption for the higher applied magnetic field ($B > 100$ G). Those matrix elements are not negligible for low magnetic field: in fact, they account for our factor of 2.7 discrepancy between the secular and non-secular calculations. Thus, the applied magnetic field affects the amount of noise: the higher the applied magnetic field, the less noise as the off-diagonal terms become insignificant. This theoretical result agrees with experimental reports [50, 51].

2. Surface impurity interactions

2.1. Model

We first calculate the magnetic field noise from the surface impurity interactions. The magnetic field noise from the surface impurities has two sources: (a) fluctuations associated with an energy transfer at the spin precession frequency

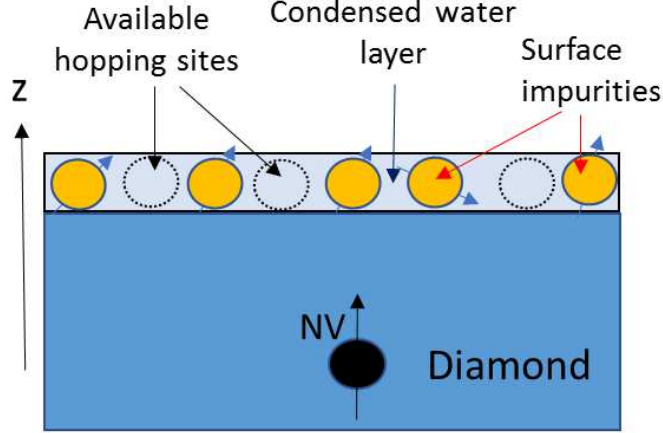


Figure 1: Our surface impurity model. Paramagnetic surface impurities are absorbed on the condensed water monolayer of hydrogen (H-), oxygen (O-), and fluorine (F-) terminated surfaces. These impurities can hop around among the terminated surface sites.

and (b) fluctuations due to spin flip induced when the impurity hops to a new termination site. Fluctuations of both types affect the dipole-dipole interactions between the impurities and the NV centers, and lead to noise.

As shown in Fig. 1, we model the paramagnetic surface impurities in the condensed thin layer of water on hydrogen (H-), oxygen (O-), and fluorine (F-) terminated systems. These impurities can move around randomly (“hop”) among the termination sites.

The Hamiltonian of the system is [37]:

$$H = H_0 + \hbar \left(\hat{\boldsymbol{\Omega}}_B + \hat{\boldsymbol{\Omega}}_{imp} \right) \cdot \mathbf{S}. \quad (1)$$

Here H_0 is the free Hamiltonian for the NV center and surface impurity electrons. The NV electron spin precession due to the applied external magnetic field is expressed in

$$\boldsymbol{\Omega}_B = \mu_B g_e(\parallel, \perp) \mathbf{B} = \frac{\mu_B}{\hbar} \left[g_e^\parallel B_z \hat{\mathbf{z}} + g_e^\perp (B_x \hat{\mathbf{x}} + B_y \hat{\mathbf{y}}) \right], \quad (2)$$

in which $\mathbf{B}(x, y, z)$ is the external magnetic field and g_e^\parallel and g_e^\perp are the electron g -factor tensors. The term $\boldsymbol{\Omega}_{imp} \cdot \mathbf{S}$ models the interaction between the NV center electron spins and the surface impurity electron spins, via

$$\boldsymbol{\Omega}_{imp} = \sum_{n=1}^N A_n \left[S_{n,z}^{(imp)} \hat{\mathbf{z}} + \frac{1}{\lambda} \left(S_{n,x}^{(imp)} \hat{\mathbf{x}} + S_{n,y}^{(imp)} \hat{\mathbf{y}} \right) \right]. \quad (3)$$

Here $S_n^{(imp)}$ is the spin operator of the n -th surface impurity electron, A_n is the coupling constant between the NV center electron and the n -th surface

impurity electron, and λ is the anisotropy parameter. The total number of surface impurity electrons is N . We take the z -axis to be the normal vector to the surface plane and place the origin at the NV center. We write the overall effective frequency as a linear superposition of $\mathbf{\Omega}_B$ and $\mathbf{\Omega}_{imp}$ which we define as $\mathbf{\Omega} \equiv (\mathbf{\Omega}_B + \mathbf{\Omega}_{imp})$.

We take a semiclassical approach by using the Langevin method applied to the Bloch equation [35, 38], we describe the stochastic dynamics of the spin fluctuation $S(t)$ as

$$\frac{\partial \mathbf{S}(t)}{\partial t} = \mathbf{\Omega} \times \mathbf{S}(t) - \sum_{j=1}^N [W_{oj} \mathbf{S}(t) - W_{jo} \mathbf{S}(t)] - \nu_s \mathbf{S}(t). \quad (4)$$

Here ν_s is the impurity electron spin relaxation frequency. It is the reciprocal of τ_s , the relaxation time due to the environment, excluding the NV center spin-impurity spin interaction. The quantities W_{jo} are the impurity hopping rates from the site j to site o , where o is located right above the NV center.

2.2. Correlation and noise spectrum

The noise spectrum may be written in terms of the two-time correlation function as

$$S(\omega) = \int \langle S(t+\tau) S(t) \rangle e^{i\omega\tau} d\tau. \quad (5)$$

Defining $W_0 = 1/\tau_c$ where τ_c is the impurity electron correlation time for the given surface terminating atom and using Eqs. (4) and (5) together with spin fluctuation theory [35, 38, 52, 53], we obtain

$$(-i\omega + \nu_s + W_0) \mathbf{S} + \mathbf{S} \times \mathbf{\Omega} = \frac{1}{4} + \frac{W_0}{N} \mathbf{S}(t). \quad (6)$$

The cross product in Eq. (6) can be represented using $\mathbf{S} \times \mathbf{\Omega} = \sum_{j,k} \epsilon_{ijk} \Omega_{ij} S_{ij}$

where ϵ_{ijk} is the Levi-Civita tensor and $i, j, k = x, y, z$. Then, we obtain the noise spectrum

$$S(\omega) = \frac{\tau_\omega}{4} \frac{\mathcal{A}(\tau_\omega)}{1 - W_0 \tau_\omega \mathcal{A}(\tau_\omega)} + c.c., \quad (7)$$

$$\tau_\omega = \frac{1}{\nu_s + W_0 - i\omega}, \quad (8)$$

and

$$\mathcal{A}(\tau_\omega) = \frac{1}{N} \sum_i^N \frac{1 + \Omega_{iz}^2 \tau_\omega^2}{1 + \Omega_i^2 \tau_\omega^2}. \quad (9)$$

In general the spin-spin interaction will be anisotropic because of the dipolar interaction. However, the anisotropic part is averaged out in the molecular motion in solution, and so we can focus on the fluctuations in the z -direction. The average contributions of the impurities to the spin precession, Ω_i , in each

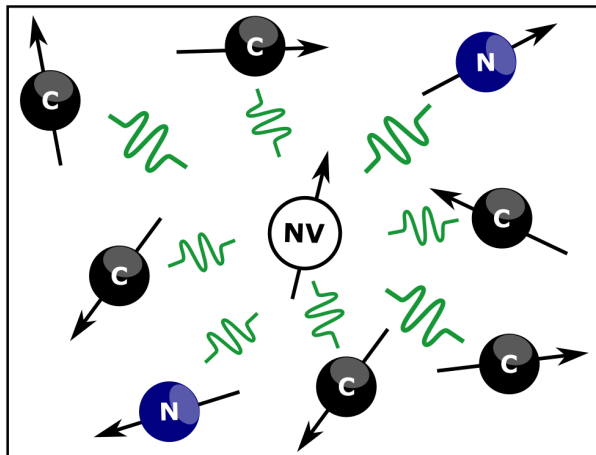


Figure 2: The model of interacting NV center and impurities. Carbon-13 is shown black, nitrogen in blue, and the dipole-dipole interaction between the impurities and the NV center in green. The spins of the impurities are randomly oriented.

direction along the surface will obey a Gaussian distribution, $\mathcal{F}(\Omega_{imp})$, giving us [35]

$$\mathcal{F}(\Omega_{imp}) = \frac{\lambda}{(\sqrt{\pi}\delta_e)^3} \exp\left(-\frac{\Omega_{imp}^2}{\delta_e^2}\right), \quad (10)$$

where δ_e is the Larmor frequency of the NV center electron affected by the impurity electron spin field and for electrons $\lambda = 1$. Then $\mathcal{A}(\tau_\omega)$ becomes

$$\mathcal{A}(\tau_\omega) = \frac{1}{3} + \frac{4}{3(\delta_e\tau_\omega)^2} - \frac{4\sqrt{\pi} \exp\left[\frac{1}{\delta_e^2\tau_\omega^2}\right]}{3(\delta_e\tau_\omega)^3} \text{erfc}\left(\frac{1}{\delta_e\tau_\omega}\right). \quad (11)$$

3. Bulk impurity interactions

3.1. Model

We now turn to the magnetic field noise due to bulk impurity interactions. The main bulk impurities responsible for magnetic field noise are naturally occurring carbon-13 isotopes and nitrogen atoms that are left over from the process of creating the NV centers. Magnetic field noise arises from the dipole-dipole interaction between the nuclear spins of the bulk impurities and the electron spin of the NV center diamond. The free electron in the NV center feels the magnetic field generated by the randomly oriented nuclear spins of the bulk impurities. The nuclear spin magnetic field fluctuates causing the electron to precess. The model is shown in Fig. 2.

The Hamiltonian of this model is

$$H = H_0 + H_{\text{II}} + H_{\text{SI}}. \quad (12)$$

Here H_0 includes the free Hamiltonian, the zero field splitting term, spin orbit (SO) coupling term, and the Zeeman term. It has been reported that zero field splitting decouples the interaction between the NV center electron spin and the spin bath and maintains coherence in NV center applications [54], thus, the noise contribution from the zero field splitting is not significant, and we have incorporated the term into H_0 . H_{II} reflects the magnetic dipole-dipole hyperfine interactions among the bulk impurities; and H_{SI} accounts for the dipole-dipole hyperfine interactions between the NV center and the bulk impurities. The two interaction Hamiltonians H_{II} and H_{SI} are mainly responsible for generating magnetic noise. The Hamiltonian for the magnetic dipole-dipole interactions among the bulk impurities is

$$H_{\text{II}} = \sum_{j < i} \frac{b}{r_{ij}^3} \left[\vec{I}_i \cdot \vec{I}_j - 3 \frac{(\vec{I}_i \cdot \vec{r}_{ij})(\vec{r}_{ij} \cdot \vec{I}_j)}{r_{ij}^2} \right]. \quad (13)$$

Here

$$b = \frac{\mu_0 \mu_{\text{I}}^2}{4\pi\hbar}; \quad (14)$$

I_i and I_j are the nuclear spin operators for the i th and j th nuclear spins in the cluster, μ_0 is the vacuum permeability, μ_{I} is the nuclear magnetic moment, and r_{ij} is the distance between the nuclear spins.

The Hamiltonian for the dipole-dipole interaction between the NV center electron spin, \vec{S} and the bulk impurity nuclear spins, \vec{I}_i with $i = 1 \dots N$, is described by

$$H_{\text{SI}} = \sum_i \frac{a}{R_i^3} \left[\vec{S} \cdot \vec{I}_i - 3 \frac{(\vec{S} \cdot \vec{R}_i)(\vec{R}_i \cdot \vec{I}_i)}{R_i^2} \right], \quad (15)$$

where

$$a = \frac{\mu_0 \mu_{\text{e}} \mu_{\text{I}}}{4\pi\hbar}, \quad (16)$$

μ_{e} is the electron magnetic moment, and R_i is the distance between the NV center and the impurity spin.

3.2. Correlation and noise spectrum

3.2.1. Two-time correlation for one cluster

We follow Hall, *et al.* [55] and use the correlated-cluster expansion method to calculate the two-time correlation of the magnetic field fluctuations. We set the z -direction to be the crystal axis. The magnetic field operator of the impurity cluster felt by the NV center can be written in terms of the axial components of the nuclear dipole-dipole hyperfine interactions as

$$\hat{B} = \sum_{n=1}^k (T_{zx}^n I_x^n + T_{zy}^n I_y^n + T_{zz}^n I_z^n), \quad (17)$$

where T_{zj} with $j = x, y, z$ is the hyperfine interaction tensor, I is the impurity nuclear spin, and k is the number of spins within the cluster. When the applied magnetic field is large, the secular (S) approximation which is similar to the rotating-wave approximation allows us to neglect the non energy conserving off-diagonal terms of the nuclear dipole-dipole Hamiltonian (Eq. (13)). For small applied magnetic fields, the non-secular method (NS), all possible terms of Eq. (13) must be considered. For the purposes of this study we consider anything below 1 G to be low fields and anything above 100 G to be large fields.

Starting from Eq. (17) we calculate the two-time correlation function of the magnetic field of the impurity cluster for both the secular and non-secular approximation. Here we consider a cluster of $k = 2$ spins because Hall *et al.* [55] shows that clusters of $k > 2$ spins exhibit identical properties as the $k = 2$ spin cluster due to rapid falloff of dipole-dipole coupling strength. In the secular approximation, the magnetic field two-time correlation along the crystal axis can then be written as

$$\langle B(t)B(0) \rangle_S = T_{z,1}^2 + T_{z,2}^2 - [T_{z,1} - T_{z,2}]^2 \sin^2 \left(\frac{B_{12}t}{2} \right); \quad (18)$$

in the non-secular calculation, the autocorrelation function of the axial magnetic field will be

$$\langle B(t)B(0) \rangle_{NS} = (T_{z,1}^2 + T_{z,2}^2) \left[1 - \frac{3}{4} \sin^2 \left(\frac{3B_{12}t}{4} \right) \right]. \quad (19)$$

Here $B_{12} = b/r_{12}^3 [1 - 3 \cos^2(\theta_{12})]$ is the axial flipping rate of the cluster magnetic field between being parallel or anti-parallel to the z -axis. B_{12} is determined by r_{12} the distance between the two spins of the cluster, and θ_{12} the angle between r_{12} and the z -axis.

3.2.2. Two-time correlation function for N clusters

To generalize the result of Sec. 3.2.1 to the N cluster case, we must sum over all the clusters in the system. Since the dynamics of the clusters are stochastic in nature and their magnetic field strengths will depend on their radial distribution, we use a probability density function of finding a fixed number n' of spins on a concentric sphere within a distance r' of the NV center. The probability density function for considering a single cluster will follow a Poisson distribution and will be as follows,

$$p(r') = (4\pi n' r'^2) \exp \left[-\frac{4\pi n' r'^3}{3} \right]. \quad (20)$$

Now if we consider the joint probability distribution for N clusters, the probability density function for N clusters with k spins will become,

$$P(r', \dots, r'_k) = \prod_{j=1}^k p_r(r'_j), \quad (21)$$

where $p_r(r'_j)$ is the probability density function of a cluster at a distance r'_j where $j = 1 \dots k$. With Eqs. (20) and (21), we obtain

$$P(r') = \frac{(4\pi n' r_k'^2)}{(k-1)!} \left(\frac{4\pi n' r_k'^3}{3} \right)^{k-1} \exp \left[-\frac{4\pi n' r_k'^3}{3} \right]. \quad (22)$$

Then the two-time correlation function of the system is as follows

$$C(t) = \sum_{i=1}^N \langle B(t)B(0) \rangle_i P(r'), \quad (23)$$

and the noise spectrum is

$$S(\omega) = \int_0^t C(t') \cos(\omega t') dt'. \quad (24)$$

Plugging in Eqs. (18) and (19) to Eq. (23), we can work out our magnetic field correlation functions for N clusters and have the following form

$$C_S(t) = \frac{8}{5} \left(\frac{4}{3} \pi a n \right)^2 \left[1 - \frac{1}{3} M(t) \right], \quad (25)$$

for the secular approximation and

$$C_{NS}(t) = \left(\frac{8}{3} \pi a n \right)^2 \left[1 - N(t) \right], \quad (26)$$

for the non-secular case. Here n is the number density of the impurities, and $M(t)$ and $N(t)$ are the cluster magnetization functions of the system and are given by [55]

$$M(t) = \frac{4\pi \sqrt[3]{6}}{\Gamma(\frac{8}{3})} (\pi b n t)^{5/3} - \frac{8\pi}{\sqrt{3}\Gamma(\frac{4}{3})} (\pi b n t)^2, \quad (27)$$

and

$$N(t) = \left(\frac{4}{9} \pi^2 b n t \right), \quad (28)$$

where Γ is the gamma function. Plugging Eqs. (25) and (26) into Eq. (24), the noise spectrum becomes,

$$S(\omega)_S = \int_0^t \frac{8}{5} \left(\frac{4}{3} \pi a n \right)^2 \left[1 - \frac{1}{3} M(t') \right] \cos(\omega t') dt', \quad (29)$$

in the secular approximation and

$$S(\omega)_{NS} = \int_0^t \left(\frac{8}{3} \pi a n \right)^2 \left[1 - N(t') \right] \cos(\omega t') dt', \quad (30)$$

in the non-secular approximation.

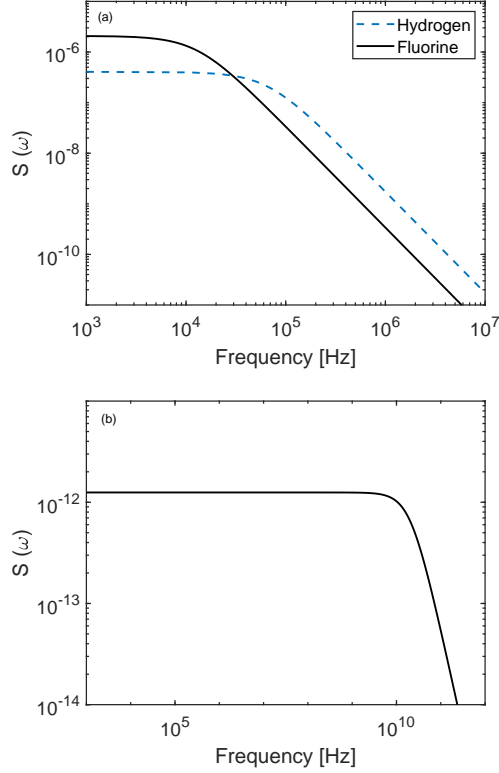


Figure 3: Noise spectrum of (a) F- and H-terminated surfaces and (b) O-terminated surface with $N = 10^6$ paramagnetic surface impurities. The O-terminated system has much less noise than the H- and F- terminated systems. This is because oxygen electron spins have an extremely short spin precession relaxation time.

4. Results and discussions

4.1. Surface impurity noise

Figure 3 (a) and (b) show the calculated noise spectral density for H-, O-, and F- terminated NV center diamonds. The constant noise floor at low frequency comes from the electron spins of the surface impurities and the NV center randomly precessing and trying to relax to an equilibrium state. At high frequencies, the noise spectrum follows a power law.

4.1.1. Spin flip noise and spin precession noise

At low frequencies, F-terminated surface generates the highest noise of the three termination systems. At around 40 kHz and above, the H-terminated surface has higher noise than the F-terminated surface. The O-terminated surface has much less noise than H- and F-terminated surfaces in the practical oper-

ational frequency range ($10^3 - 10^8$ Hz). At low frequencies ($< 10^4$ Hz), the difference is as much as 5 or 6 orders of magnitude.

This huge difference in magnetic field noise can be attributed to the very short (~ 7.5 ps) spin-lattice relaxation time of the impurity electron spin in the O-terminated surface compared to that of H- and F-terminated surface, where the spin-lattice relaxation times are on the order of microseconds: $13 \mu\text{s}$ for hydrogen and $300 \mu\text{s}$ for fluorine. A short relaxation time ($\delta_e < \nu_s$) leads to a short impurity-impurity correlation time, and thus, the noise is purely due to spin flip fluctuations since the much quicker spin-precession will not contribute to noise while they are correlated. On the other hand, long relaxation time ($\delta_e > \nu_s$) leads to a long impurity-impurity spin correlation time, which in turn adds the effect of spin-precession fluctuation noise to the spin flip fluctuation noise. The huge differences in the amount of noise by termination suggest that spin precession fluctuations seem to dominate the magnetic field noise.

4.1.2. Impurity number and noise

The effective relaxation time is limited by the faster of the spin flips and the hopping rates. The number of impurities affects only the hopping rate. Thus if $\nu_s < W_0$, the effective relaxation time is limited by the hopping rate, while if $\nu_s > W_0$, the relaxation time is limited by the spin flip process. The hopping induced spin flip rate depends on the number of impurity spins. For O-terminated surfaces, $\nu_s \gg W_0$, and so the noise is not affected by the number of impurities. However, H- and F-terminated surfaces are different. At low N , the relaxation times of H- and F-terminated surfaces are determined by the hopping rate, since $\nu_s < W_0$ in this regime. At high N , the situation is reversed: the spin flip rate dominates the relaxation times, since $\nu_s > W_0$. For H-terminated surfaces, the transition between the low N and high N regimes occurs around $N = 10^6$.

Figure 4 shows the noise at $\omega = 10^3$ Hz (i.e., the largest noise value since the low frequency region has almost flat region in the noise spectrum as seen in Fig. 4) vs. the number of impurity spins for H- and O-terminated surfaces. In O-terminated systems, where the relaxation time is limited by spin flips, the noise spectrum exhibits no impurity number dependence. In H-terminated systems, however, we see the transition from the low- N regime in which relaxation time is controlled by hopping ($\nu_s < W_0$) to the high- N regime in which spin flips control the relaxation time ($\nu_s > W_0$). This transition indeed occurs around $N \sim 10^6$ as the relation between ν_s and W_0 shifts to $\nu_s > W_0$.

4.2. Bulk impurity noise spectrum

Figure 5 shows the noise spectrum produced by (a) carbon-13 and (b)nitrogen impurities, calculated in the non-secular method. The results show that the noise due to dipole-dipole interactions between the NV center and carbon-13 impurities is roughly two orders of magnitude greater than that the noise from the nitrogen impurities. The reason for the difference is number density, which affects the noise spectrum in two ways. (1) Because the number density of

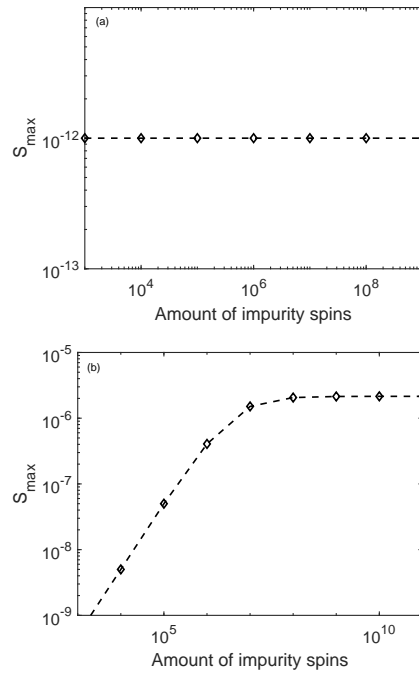


Figure 4: Noise at $\omega = 10^3$ Hz (the largest value of the noise spectrum) vs. the number of impurities for (a) O-terminated surface and (b) H-terminated surface. Calculated values are shown in diamonds and dotted lines are interpolation. The the noise spectrum is unaffected by the number of impurities in the O-terminated surface, while in the H-terminated surface, the amount of noise increases with the number of impurities until reaching a relaxation time controlling mechanism transition occurs at about $N = 10^6$.

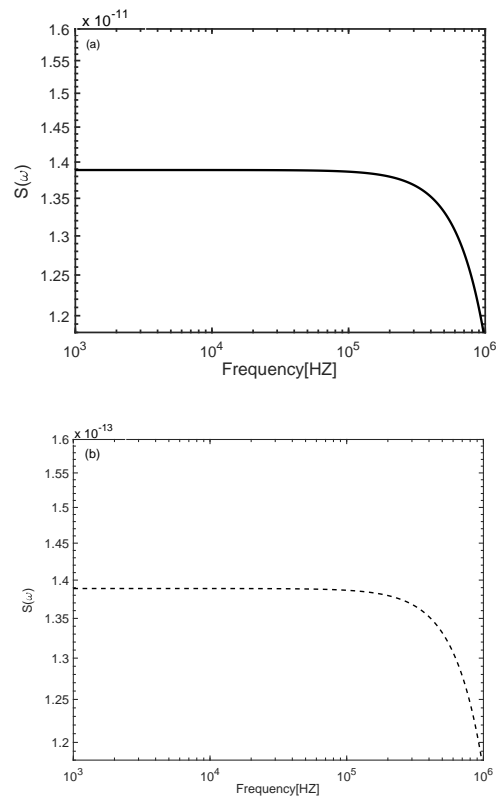


Figure 5: magnetic noise spectrum for (a) carbon-13 impurities and (b) nitrogen impurities. The calculation is done at low applied magnetic field, using the non-secular method. The assumed number density is 10^{19} atoms/cm³ for carbon-13 and roughly 10^{18} atoms/cm³ for nitrogen. These are typical experimental number densities. The carbon-13 noise is roughly 100 times greater than that of nitrogen.

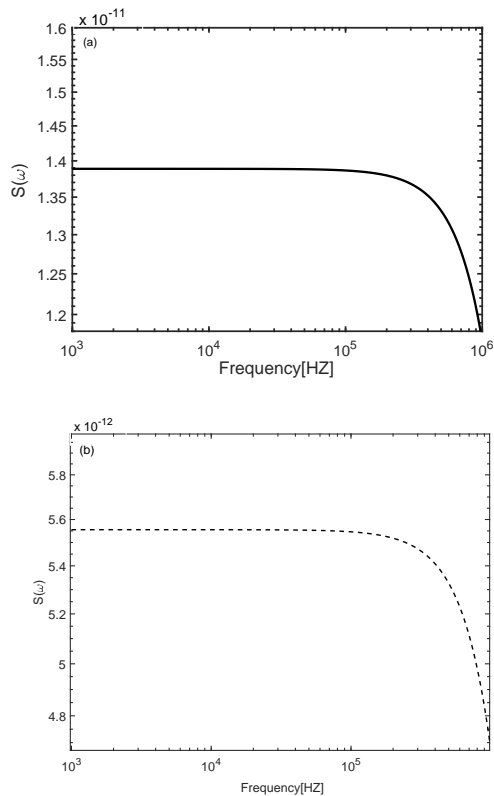


Figure 6: Magnetic noise spectrum from carbon-13 impurities calculated with (a) the secular approximation and (b) the exact non-secular method. The noise is three times larger in the non-secular calculation. Thus the secular approximation underestimates the noise at low applied magnetic field.

carbon-13 is greater than that of nitrogen, the average interaction distance between carbon-13 atoms and the NV centers is smaller than the average nitrogen-NV center interaction distance. Consequently, the carbon-13 nuclear spins have stronger interactions with the NV centers, generating more noise. (2) A greater number density of impurities increases the number of nuclear spin flip-flops. These spin flip-flops perturb the free electron in the NV center, causing the electron to precess. The precession, in turn, leads to greater fluctuations of the NV center electron spin state. The maximum noise of $S(\omega)$ is related to the number density by a power-law of $S(\omega) \propto n^2$.

4.2.1. Secular approximation vs. non-secular method

Most calculations of bulk impurity interactions tend to use the secular approximation, because it simplifies the analysis. However, at low applied magnetic field, the secular approximation is inaccurate. To demonstrate this, we calculate the noise spectrum at low magnetic field using both the secular ap-

proximation and non-secular methods. Figure 6 shows the two calculations for the noise spectrum from interactions of NV centers with carbon-13. We see that the secular approximation underestimates the amount of noise by a factor of 2.7.

The reason for the underestimate is as follows. There is a degeneracy between the $m_s = +1$ and $m_s = -1$ ground states at zero applied magnetic field, which is broken by applying a magnetic field. If the applied magnetic field is high, the split is large enough so that the off-diagonal terms of the nuclear dipole-dipole interaction Hamiltonian (Eq. (13)) can be neglected, and thus, the secular approximation is valid. However, at low applied magnetic field, these off-diagonal elements are not negligible. In fact, they account for our factor of 2.7 discrepancy between the secular and non-secular calculations. Some experimentalists deliberately work at high applied magnetic fields so that the secular approximation will be valid for their experiments [50, 51].

4.3. Surface vs. bulk impurity noise

Unlike surface impurities, bulk impurities are located at fixed positions, thus there is no hopping between different sites. As a result, bulk impurity noise is purely spin flip noise. On the other hand, the surface impurities can hop from site to site resulting in possibly having both spin flip noise and spin precession noise or spin flip noise only depending on either the spin flip rate or the hopping rate controlling the effective relaxation time as discussed in Sec. 4.1. We have seen that an O-terminated surface, that has only spin flip noise due to short relaxation time, produces 5 to 6 orders of magnitude less noise at low frequency range than H- and F-terminated surfaces that have both spin precession noise and spin flip noise in the low frequency range of $< 10^4$ Hz. Comparing the noise between surface noise and bulk noise, we notice that bulk noise is about the same or even less noise than the O-terminated, which confirms that the spin precession noise is indeed the major magnetic noise source.

However, for the bulk impurities, the impurity number density also has a significant effect on noise as impurities are at fixed position and the interaction strength changes with the density while for the surface impurities, the impurity numbers increase noise as long as the relaxation is limited by the hopping rate as the impurity number changes the hopping rate.

5. Conclusions

We have analytically and numerically investigated the magnetic noise from paramagnetic surface and bulk impurities. For surface impurities, we studied the interactions between the paramagnetic surface impurity electron spins and the NV center electron spins. In such systems, different species can terminate the dangling bonds at the diamond surface, and the impurities are dissolved in a condensed thin layer of water. We studied three different surface terminations; hydrogen, oxygen, and fluorine. Applying the Langevin method to the Bloch equation, we calculated the spin-spin noise spectrum.

Our results show that there are two mechanisms that contribute to noise: spin flip fluctuations and spin precession fluctuations. A short relaxation time leads to a short impurity-impurity spin correlation time resulting in a spin flip fluctuation noise only. On the other hand, a long relaxation time leads to a long impurity-impurity spin correlation time, which results in activating another effect of spin-precession fluctuation noise to the already existing spin flip fluctuation noise. Thus, an O-terminated surface, for which the spin-lattice relaxation time is very short, have only the spin flip fluctuation noise while H- and F-terminated surfaces, with a longer spin-lattice relaxation time, have both spin flip and precession fluctuation noise. The spin precession fluctuation noise is much larger than the spin flip fluctuation noise, dominating the magnetic field noise in NV center diamonds.

The effective relaxation time of impurities is limited by the faster of either the spin flip rate or the hopping rate. The reaction limited nature of the bonding between the hopping terminating atoms and the dangling bond allow most of the sites above and near the NV center to be occupied. At this point, the terminating atoms with long relaxation times are still generating spin precession noise which generates more noise than spin flips due to hopping. At high frequencies (short time scales), the dominating presence of the spin precession is not fully felt as the terminating atoms have not had the time to make the energetically stable bond with the dangling bond. The number of impurities affects only the hopping rate. Since the relaxation time of an O-terminated surface is determined by the spin flip rate, it is not affected by the change in the number of impurities. On the other hand, the relaxation times of H- and F-terminated surfaces are controlled by either the hopping rate, if $N < 10^6$, or the spin flip rate, if $N > 10^6$ and the transition between two control mechanism can be seen clearly by plotting the maximum noise vs impurity.

The bulk magnetic noise is caused by the bulk impurity nuclear spin interactions with the NV center electron spin. The major bulk impurities of the system are carbon-13 and the leftover nitrogen from implantation. We used the correlated-cluster expansion to calculate the magnetic field noise from the nuclear spin flip fluctuations. We numerically evaluated the noise spectrum for both the carbon-13 and the nitrogen impurities at low magnetic fields. We find that the noise from carbon-13 was roughly two orders of magnitude larger than that from nitrogen. We attribute this difference to number density. The number density affects the noise spectrum through two physical mechanisms: the distance between the impurities and the NV center, which affects the interaction strength, and the spin flip rate. Carbon-13 has greater number density than nitrogen, and hence produces greater noise. Different grade of NV-center environments are used in experiment from 99.999% carbon-12 to $> 50\%$ enriched carbon-13. Plotting the maximum noise versus number density, a linear increase as the number density increases is clearly seen.

We also examined the applicability of the secular approximation that is commonly used to estimate the noise. We find that the secular approximation underestimates the amount of noise when the applied magnetic field is low. This is related to lifting the degeneracy of $m_s = \pm 1$ states. At high applied

magnetic field, the split is large enough that some of the off-diagonal terms of the nuclear dipole-dipole interaction matrix can be neglected, and thus the secular approximation is valid. However, at low magnetic field, the off-diagonal elements are not negligible, and must be considered in the noise calculations.

Comparing the surface and bulk impurity noise spectra, surface impurities with O-terminated surface and bulk impurities have significantly less noise than the H- and F-terminated surfaces due to only having spin flip noise and no spin precession noise. It might be possible to employ research techniques similar to the spin noise spectroscopy done for gallium-arsenide to distinguish spin precession noise from spin flip noise [56], which could help indicate terminating atoms with the desirable rapid spin precession relaxation. However, it is beyond the scope of this paper.

The inclusion of the spin precession in our model has given us insight into a mechanism other models have looked over. For the bulk impurities, the impurity number density also has a significant effect by changing the interaction strength. For the surface impurities, the impurity numbers increase noise as long as the relaxation is limited by the hopping rate as the impurity number changes the hopping rate.

We thank Jonathan Tannenhauser for the valuable input. This work is supported by NSF DMR-1505641.

References

- [1] G. Balasubramanian, P. Neumann, D. Twitchen, M. Markham, R. Kolesov, N. Mizuochi, J. Isoya, J. Achard, J. Beck, J. Tissler, V. Jacques, P. R. Hemmer, F. Jelezko, and J. Wrachtrup, Ultralong spin coherence time in isotopically engineered diamond, *Nat. Mater.* **8**, 383 (2009).
- [2] Bonato, C., Blok, M. S., Dinani, H. T., Berry, D. W., Markham, M. L., Twitchen, D. J., & Hanson, R., Optimized quantum sensing with a single electron spin using real-time adaptive measurements, *Nature Nanotech* **11**, 247 (2016).
- [3] Dolde, F., Fedder, H., Doherty, M. W., Nobauer, T., Rempp, F., Balasubramanian, G., Wrachtrup, Electric-field sensing using single diamond spins, *Nature Physics* **7**, 459 (2011).
- [4] V. M. Acosta, E. Bauch, M. P. Ledbetter, A. Waxman, L.-S. Bouchard, and D. Budker, Temperature Dependence of the Nitrogen-Vacancy Magnetic Resonance in Diamond, *Phys. Rev. Lett.* **104**, 070801 (2010).
- [5] David M. Toyli, Charles F. de las Casas, David J. Christle, Viatcheslav V. Dobrovitski, and David D. Awschalom, Fluorescence thermometry enhanced by the quantum coherence of single spins in diamond, *Proc. Natl Acad. Sci. USA* **110**, 8417 (2013).

- [6] Kejie Fang, Victor M. Acosta, Charles Santori, Zhihong Huang, Kohei M. Itoh, Hideyuki Watanabe, Shinichi Shikata, and Raymond G. Beausoleil, High-Sensitivity Magnetometry Based on Quantum Beats in Diamond Nitrogen-Vacancy Centers, *Phys. Rev. Lett.* **110**, 130802 (2013).
- [7] Thomas Wolf, Philipp Neumann, Kazuo Nakamura, Hitoshi Sumiya, Takeshi Ohshima, Junichi Isoya, and Jörg Wrachtrup, Subpicotesla Diamond Magnetometry, *Phys. Rev. X* **5**, 041001 (2015).
- [8] Romana Schirhagl, Kevin Chang, Michael Loretz, and Christian L Degen, Nitrogen-Vacancy Centers in Diamond: Nanoscale Sensors for Physics and Biology, *Annu. Rev. Phys. Chem.* **65**, 83 (2014).
- [9] Jeronimo R Maze, Adam Gali, Emre Togan, Yiwen Chu, Alexei Trifonov, Efthimios Kaxiras, and Mikhail D Lukin, Properties of nitrogen-vacancy centers in diamond: the group theoretic approach, *New J. Phys.* **13**, 025025 (2011).
- [10] D. Le Sage, K.Arai, D.R. Glenn, S.J. DeVience, L.M. Pham, L.Rahn-Lee, M.D. Lukin, A.Yacoby, A. Komeili, and R.L. Walsworth, Optical magnetic imaging of living cells, *Nature (London)* **496**, 486 (2013).
- [11] D.A. Simpson, R. G. Ryan, L. T. Hall, E. Panchenko, S. C. Drew, S. Petrou, P. S. Donnelly, P. Mulvaney, and L. C. L. Hollenberg, Electron paramagnetic resonance microscopy using spins in diamond under ambient conditions, *Nat. Commun.* **8**, 458 (2017).
- [12] Zhou, T. X, Stohr, and R. J, Yacoby, A., Scanning diamond NV center probes compatible with conventional AFM technology, *Appl. Phys. Lett.* **111**, 163106 (2017).
- [13] Su, L. J., Fang, C. Y., Chang, Y. T., Chen, K. M., Yu, Y. C., Hsu, J. H., Chang, H. C., Creation of high density ensembles of nitrogen-vacancy centers in nitrogen-rich type Ib nanodiamonds, *Nanotechnology* **24**, 315702 (2013).
- [14] Georg Kucsko, PC Maurer, Norman Ying Yao, Michael Kubo, HJ Noh, PK Lo, Hongkun Park, and Mikhail D Lukin, Nanometre-scale thermometry in a living cell, *Nature* **500**, 54 (2013).
- [15] Taras Plakhotnik, Marcus W Doherty, Jared H Cole, Robert Chapman, and Neil B Manson, All-optical thermometry and thermal properties of the optically detected spin resonances of the NV(-) center in nanodiamond, *Nano Lett.* **14**, 4989 (2014).
- [16] S. J. DeVience, L. M. Pham, I. Lovchinsky, A. O. Sushkov, N. Bar-Gill, C. Belthangady, F. Casola, M. Corbett, H. Zhang, M. Lukin, H. Park, A. Yacoby, and R. L. Walsworth, Nanoscale NMR spectroscopy and imaging of multiple nuclear species, *Nat. Nanotech.* **10**, 129 (2015).

- [17] T. Staudacher, F. Shi, S. Pezzagna, J. Meijer, J. Du, C. A. Meriles, F. Reinhard, and J. Wrachtrup, Nuclear Magnetic Resonance Spectroscopy on a (5-Nanometer) 3 sample volume, *Science* **339**, 561 (2013).
- [18] I. Lovchinsky, J. D. Sanchez-Yamagishi, E. K. Urbach, S. Choi, S. Fang, T. I. Andersen, K. Watanabe, T. Taniguchi, A. Bylinskii, E. Kaxiras, P. Kim, H. Park, and M. D. Lukin, Magnetic resonance spectroscopy of an atomically thin material using a single-spin qubit, *Science* **355**, 503 (2017).
- [19] D. R. Glenn, K. Lee, H. Park, R. Weissleder, A. Yacoby, M. D. Lukin, H. Lee, R. L. Walsworth, and C. B. Connolly, Single-cell magnetic imaging using a quantum diamond microscope, *Nat. Methods* **12**, 736 (2015).
- [20] R. R. Fu *et al*, Solar nebula magnetic fields recorded in the Semarkona meteorite *Science* **346**, 1089 (2014).
- [21] P. Kehayias, M. Mrózek, V. M. Acosta, A. Jarmola, D. S. Rudnicki, R. Folman, W. Gawlik, and D. Budker, Microwave saturation spectroscopy of nitrogen-vacancy ensembles in diamond, *Phys. Rev. B* **89**, 245202 (2014).
- [22] Gopalakrishnan Balasubramanian, Andrii Lazariev, Sri Ranjini Arumugam, and De-wen Duan, Nitrogen-Vacancy color center in diamond-emerging nanoscale applications in bioimaging and biosensing, *Curr. Opin. Chem. Biol.* **20**, 69 (2014).
- [23] Changbiao Li, Zihai Jiang, Yiqi Zhang, Zhaoyang Zhang, Feng Wen, Haixia Chen, Yanpeng Zhang, and Min Xiao, Controlled Correlation and Squeezing in $\text{Pr}^{3+}:\text{Y}_2\text{SiO}_5$ to Yield Correlated Light Beams, *Phys. Rev. Appl.* **7**, 014023 (2017).
- [24] Huanrong Fan, Faizan Raza, IrfanAhmed, Kangkang Li, Habib Ullah, and Yanpeng Zhang, Three-type Fano interference controlled by the phase transition of $\text{Eu}^{3+}/\text{Pr}^{3+}:\text{YPO}_4$, *New J. Phys.* **22**, 093008 (2020).
- [25] Faizan Raza, Huanrong Fan, Habib Ullah, Faisal Nadeem, Hasnain Ali, Jinyang Li, and Yanpeng Zhang, Optical transistor and router application of Autler–Townes-splitting in various solid atomic-like media, *Opt. Lett.* **45**, 240-243 (2020).
- [26] Philip Chrostoski, H.R. Sadeghpour, and D.H. Santamore, Electric noise spectra of a near-surface nitrogen vacancy center diamond with a protective layer, *Phys. Rev. Appl.* **10**, 064056 (2018).
- [27] V. Y. Osipov, A. Shames, and A. Y. Vul', Exchange coupled pairs of dangling bond spins as a new type of paramagnetic defects in nanodiamonds, *Physica (Amsterdam) B* **404**, 4522 (2009).
- [28] R. C. Bansal, F. J. Vastola, and P. L. Walker, Kinetics of chemisorption of oxygen on diamond, *Carbon* **10**, 443 (1972).

- [29] J. P. Tetienne, T. Hingant, L. Rondin, A. Cavaillès, L. Mayer, G. Dantelle, T. Gacoin, J. Wrachtrup, J. F. Roch, and V. Jacques, Spin relaxometry of single nitrogen-vacancy defects in diamond nanocrystals for magnetic noise sensing, *Phys. Rev. B* **87**, 235436 (2013).
- [30] Helena S Knowles, Dhiren M Kara, and Mete Atatüre, Observing bulk diamond spin coherence in high-purity nanodiamonds, *Nature Materials* **13**, 21 (2014).
- [31] T. Rosskopf, A. Dussaux, K. Ohashi, M. Loretz, R. Schirhagl, H. Watanabe, S. Shikata, K. M. Itoh, and C. L. Degen, Investigation of Surface Magnetic Noise by Shallow Spins in Diamond, *Phys. Rev. Lett.* **112**, 147602 (2014).
- [32] Lan Luan, Michael S. Grinolds, Sungkun Hong, Patrick Maletinsky, Ronald L. Walsworth and Amir Yacoby, Decoherence imaging of spin ensembles using a scanning single-electron spin in diamond, *Scientific Reports* **5**, 8119 (2015).
- [33] M. V. Hauf, B. Grotz, B. Naydenov, M. Dankerl, S. Pezzagna, J. Meijer, F. Jelezko, J. Wrachtrup, M. Stutzmann, F. Reinhard, and J. A. Garrido, Chemical control of the charge state of nitrogen-vacancy centers in diamond, *Phys. Rev. B* **83**, 081304(R) (2011).
- [34] Shanying Cui and Evelyn L. Hu, Increased negatively charged nitrogen-vacancy centers in fluorinated diamond, *Appl. Phys. Lett.* **103**, 051603 (2013).
- [35] M. M. Glazov and E. L. Ivchenko, Spin noise in quantum dot ensembles, *Phys. Rev. B* **86**, 115308 (2012).
- [36] M. M. Glazov, Spin noise of localized electrons: Interplay of hopping and hyperfine interaction, *Phys. Rev. B* **91**, 195301 (2015).
- [37] Ph. Glasenapp, D. S. Smirnov, A. Greilich, J. Hackmann, M.M. Glazov, F. B. Anders, and M. Bayer, Spin noise of electrons and holes in (In,Ga)As quantum dots: Experiment and theory, *Phys. Rev. B* **93**, 205429 (2016).
- [38] Melvin Lax, Classical Noise IV: Langevin Methods, *Rev. Mod. Phys.* **38**, 541 (1966).
- [39] Abdelghani Laraoui, Florian Dolde, Christian Burk, Friedemann Reinhard, Jorg Wrachtrup, and Carlos A Meriles, High-resolution correlation spectroscopy of ^{13}C spins near a nitrogen-vacancy centre in diamond, *Nature Communications* **4**, 1651 (2013).
- [40] Rabeau, J. R., Reichart, P., Tamanyan, G., Jamieson, D. N., Prawer, S., Jelezko, F., Wrachtrup, J., Implantation of labelled single nitrogen vacancy centers in diamond using ^{15}N , *Appl. Phys. Lett.* **88**, 023113 (2006).

- [41] S Pezzagna, B Naydenov, F Jelezko, J Wrachtrup, and J Meijer, Creation efficiency of nitrogen-vacancy centres in diamond, *New J. Phys.* **12**, 065017 (2010).
- [42] Mariusz Mrozek, Daniel Rudnicki, Pauli Kehayias, Andrey Jarmola, Dmitry Budker, and Wojciech Gawlik, Longitudinal spin relaxation in nitrogen-vacancy ensembles in diamond, *EPJ Quantum Technology* **2**, 22 (2015).
- [43] Susumu Takahashi, Ronald Hanson, Johan van Tol, Mark S Sherwin, and David D Awschalom, Quenching Spin Decoherence in Diamond through Spin Bath Polarization, *Phys. Rev. Lett.* **101**, 047601 (2008).
- [44] Wen Yang and Ren-Bao Liu, Quantum many-body theory of qubit decoherence in a finite-size spin bath, *Phys. Rev. B* **78**, 085315 (2008).
- [45] Nan Zhao, Sai-Wah Ho, and Ren-Bao Liu, Decoherence and dynamical decoupling control of nitrogen vacancy center electron spins in nuclear spin baths, *Phys. Rev. B* **85**, 115303 (2012).
- [46] Wen Yang and Ren-Bao Liu, Quantum many-body theory of qubit decoherence in a finite-size spin bath. II. Ensemble dynamics, *Phys. Rev. B* **79**, 115320 (2009).
- [47] Ching-Ling Teng, Heedoek Hong, Suzanne Kiihne, and Robert G. Bryant, Molecular Oxygen Spin-Lattice Relaxation in Solutions Measured by Proton Magnetic Relaxation Dispersion, *J. Magn. Res.* **148** 31-34 (2001).
- [48] Riichi Sasamori, Yoshihiro Okaue, Toshiyuki Isobe, and Yoshihisa Matsuda, Stabilization of Atomic Hydrogen in Both Solution and Crystal at Room Temperature, *Science* **16**, (1994).
- [49] H. Rager, Proton and Fluorine-Spin-Lattice Relaxation in Polycrystalline $CoSiF_6 \cdot 6H_2O$, *Z. Naturforsch.* **36a**, 637-642 (1981).
- [50] B. A. Myers, A. Ariyaratne, and A. C. Bleszynski Jayich, Double-Quantum Spin-Relaxation Limits to Coherence of Near-Surface Nitrogen-Vacancy Centers, *Phys. Rev. Lett.* **118**, 197201 (2017).
- [51] L.T. Hall, P. Kehayias, D.A. Simpson, A. Jarmola, A. Stacey, and D. Budker, Detection of nanoscale electron spin resonance spectra demonstrated using nitrogen-vacancy centre probes in diamond, *Nat. Commun.* **7**, 10211 (2016).
- [52] D. S. Smirnov, M. M. Glazov, and E. L. Ivchenko, Effect of exchange interaction on the spin fluctuations of localized electrons, *Phys. Solid State* **56**, 254 (2014).
- [53] L. Landau and E. Lifshitz, *Physical Kinetics*, (Butterworth-Heinemann, Oxford, UK, 1981).

- [54] Yuhei Sekiguchi, Yusuke Komura, Shota Mishima, Touta Tanaka, Naeko Niikura, and Hideo Kosaka, Geometric spin echo under zero field, *Nat Commun* **7**, 11668 (2016).
- [55] Liam T Hall, Jared H Cole, and Lloyd CL Hollenberg, Analytic solutions to the central-spin problem for nitrogen-vacancy centers in diamond, *Phys. Rev. B* **90**, 075201 (2014).
- [56] Ryzhov, I., Kozlov, G., Smirnov, D. et al. Spin noise explores local magnetic fields in a semiconductor. *Sci. Rep.* **6**, 21062 (2016).